

Published in final edited form as:

*Cell*. 2010 July 9; 142(1): 144–157. doi:10.1016/j.cell.2010.06.010.

## TGF- $\beta$ Signaling Specifies Axons During Brain Development

Jason J. Yi<sup>1,2</sup>, Anthony P. Barnes<sup>4,\*</sup>, Randal Hand<sup>4</sup>, Franck Polleux<sup>4</sup>, and Michael D. Ehlers<sup>1,2,3,†</sup>

<sup>1</sup>Department of Neurobiology, Duke University Medical Center, Durham, NC 27710, USA

<sup>2</sup>Department of Pharmacology and Cancer Biology, Duke University Medical Center, Durham, NC 27710, USA

<sup>3</sup>Howard Hughes Medical Institute, Duke University Medical Center, Durham, NC 27710, USA

<sup>4</sup>Neuroscience Center, Department of Pharmacology, University of North Carolina, Chapel Hill, NC 27599, USA

### Abstract

In the mammalian brain, the specification of a single axon and multiple dendrites occurs early in the differentiation of most neuron types. Numerous intracellular signaling events for axon specification have been described in detail. However, the identity of the extracellular factor(s) that initiate neuronal polarity *in vivo* is unknown. Here, we report that transforming growth factor- $\beta$  (TGF- $\beta$ ) initiates signaling pathways both *in vivo* and *in vitro* to fate naïve neurites into axons. Neocortical neurons lacking the type II TGF- $\beta$  receptor (T $\beta$ R2) fail to initiate axons during development. Exogenous TGF- $\beta$  is sufficient to direct the rapid growth and differentiation of an axon, and genetic enhancement of receptor activity promotes the formation of multiple axons. Finally, we show that the bulk of these TGF- $\beta$ -dependent events are mediated by site-specific phosphorylation of Par6. These results define an extrinsic cue for neuronal polarity *in vivo* that patterns neural circuits in the developing brain.

### Introduction

The designation of polarized cellular domains is central to tissue function in all metazoans. Among the most polarized cells, neurons of the mammalian central nervous system (CNS), exhibit asymmetry early in brain development that in turn defines the elaboration and function of all neural circuitry (Kriegstein and Noctor, 2004). In simple formulation, neurons are binary biological units with a distinction between the somatodendritic compartment, which receives and integrates synaptic inputs, and the axon, which transmits action potentials across long distances (Barnes and Polleux, 2009). To date, most of our knowledge regarding axon specification comes from *in vitro* studies using dissociated cultures of rodent hippocampal neurons. In this system, dissociated neurons initially extend several undifferentiated neurites (stages 1-2) before entering a phase of asymmetric growth (stage 3) in which a single neurite undergoes rapid elongation and becomes the axon (Craig and Banker, 1994). Numerous intracellular signaling pathways important for the transition from an unpolarized to a polarized

© 2010 Elsevier Inc. All rights reserved.

<sup>†</sup>Corresponding Author: Michael D. Ehlers, M.D., Ph.D., Department of Neurobiology, Howard Hughes Medical Institute, Duke University Medical Center, Box 3209, Durham, NC 27710, USA, Tel: (919)684-1828, FAX (919)668-0631, ehlers@neuro.duke.edu.

\*current address: Department of Pediatrics, Oregon Health and Science University, Portland, Oregon 97239, USA

**Publisher's Disclaimer:** This is a PDF file of an unedited manuscript that has been accepted for publication. As a service to our customers we are providing this early version of the manuscript. The manuscript will undergo copyediting, typesetting, and review of the resulting proof before it is published in its final citable form. Please note that during the production process errors may be discovered which could affect the content, and all legal disclaimers that apply to the journal pertain.

state have been identified (Barnes and Polleux, 2009). However, it is not known how such pathways are initiated during neuronal development.

Several extracellular factors have been proposed to initiate neuronal polarity programs (Barnes and Polleux, 2009). For example, exogenously applied brain-derived neurotrophic factor (BDNF) can activate the polarity-inducing kinase LKB1 (Baas et al., 2004) through a cAMP-dependent protein kinase (PKA) pathway leading to axon specification *in vitro* (Shelly et al., 2007). However, mice lacking BDNF (Ernfors et al., 1994; Jones et al., 1994) or its receptor TrkB (Klein et al., 1993) survive until birth and CNS neurons in these animals do not exhibit any obvious defects in axon formation (Ernfors et al., 1994; Jones et al., 1994; Klein et al., 1993). In addition, insulin-like growth factor 1 (IGF-1) has been proposed as an extracellular factor that initiates neuronal polarity in cultured hippocampal neurons *in vitro* (Sosa et al., 2006). However, the anatomical structure of the hippocampus and cerebellum, regions that express both IGF-1 and IGF receptors, are largely normal in mice lacking IGF-1 (Vicario-Abejon et al., 2004), and mice lacking IGF-1 receptors throughout the CNS have a normal lifespan with apparently intact axon tracts (Kappeler et al., 2008). Thus, other initiating factors must exist to commence neuronal polarization in the intact mammalian brain.

Among diverse extrinsic signals in the developing brain, transforming growth factor- $\beta$  (TGF- $\beta$ ) is a pleiotropic morphogen that governs a wide variety of cellular processes including cell differentiation, proliferation, apoptosis, and specification of developmental fate (Shi and Massague, 2003). Canonical TGF- $\beta$  signaling is initiated by the binding of a ligand dimer to receptor serine/threonine kinases at the cell surface. The three closely related TGF- $\beta$  ligands (TGF- $\beta$ 1-3) bind the type II TGF- $\beta$  receptor (T $\beta$ R2), which causes its recruitment to the type I TGF- $\beta$  receptor (T $\beta$ R1). The formation of this complex allows the phosphorylation of the kinase domain of T $\beta$ R1 by T $\beta$ R2, which in turn triggers both immediate and long-term cellular changes through cytoskeletal rearrangements and transcriptional responses, respectively (Shi and Massague, 2003).

*In situ* hybridization and immunohistochemical studies have demonstrated that all three TGF- $\beta$  ligands are expressed throughout mammalian CNS development (Heine et al., 1987; Mecha et al., 2008). Earliest expression is detected in neuroepithelia at E8.5, a time in which neurulation occurs (Mecha et al., 2008), and TGF- $\beta$  receptors are highly expressed in migrating neurons of the developing cortex (Tomoda et al., 1996). Both TGF- $\beta$ 1 and TGF- $\beta$ 2 ligands have been shown to promote the sprouting and elongation of neurites in dissociated hippocampal cultures (Ishihara et al., 1994), and TGF- $\beta$  signaling mediates axonal development in the *Drosophila* mushroom body (Ng, 2008). In addition, mutations in TGF- $\beta$  receptors and signaling components have been attributed to several human developmental disorders characterized by mental retardation (Gripp et al., 2000; Loeys et al., 2005). Despite these insights, the role of TGF- $\beta$  in mammalian CNS development has remained largely unexplored.

Here, we present *in vitro* and *in vivo* evidence that TGF- $\beta$  directs axon establishment in developing neurons. TGF- $\beta$  receptors are expressed in axons during embryonic development, and receptor kinase activity is required for axon formation and neuronal migration in the developing mouse neocortex. Gain-of-function and loss-of-function experiments show that the level of TGF- $\beta$  receptor activity in young neurons dictates axon number. Moreover, exogenous TGF- $\beta$  is sufficient to spatially direct the differentiation and rapid outgrowth of axons. The effect of TGF- $\beta$  signaling on axon specification and neuronal migration is dependent on the site-specific phosphorylation of the polarity protein Par6 by T $\beta$ R2. Par6 and T $\beta$ R1 exist as a complex in developing neurons, and the expression of a phosphomimetic mutant of Par6 rescues neuronal migration and restores axons in cortical neurons lacking T $\beta$ R2 *in vivo*. These results link secreted cues with the Par3/Par6 polarity complex during axon specification, and

demonstrate an obligate role for extrinsic TGF- $\beta$  signaling in establishing neuronal polarity and axonal identity in the mammalian brain.

## Results

### TGF- $\beta$ Receptors are Expressed in Axons During Neural Development

If TGF- $\beta$  is involved in axon specification, we reasoned that TGF- $\beta$  receptor expression should be evident in axons during embryonic development. We focused on E14-15 neocortex, a time when peak neurogenesis of layer 5 cortical neurons occurs (Polleux et al., 1997). Both T $\beta$ R1 and T $\beta$ R2 are highly expressed throughout the mouse neocortex, including nestin-positive radial glial progenitors (Figure 1A). Both receptor types are present at apical domains of radial glia (Figure 1B), consistent with previous findings (Murphy et al., 2004; Ozdamar et al., 2005). In addition, TGF- $\beta$  receptor labeling was present in postmitotic neurons in the cortical plate (CP), as identified by staining with the neuron-specific  $\beta$ -tubulin III marker Tuj1 (Figure 1C). Both T $\beta$ R1 and T $\beta$ R2 were found in the cell bodies of layer 6 neurons, and diffuse T $\beta$ R1 labeling was found within the intermediate zone (IZ) of the cortical wall (Figure 1C). We observed striking T $\beta$ R2 labeling along  $\beta$ -tubulin-rich fasciculations within the IZ in E14.5 animals (Figures 1C top panels and 1D), and this signal became more prominent in E18 embryos (Figure 1C, bottom panels), suggesting the pre presence of TGF- $\beta$  signaling machinery in new axons. Indeed, we simultaneously labeled the cortex with an antibody for T $\beta$ R2 and TAG1, a marker of corticofugal axons (Kawano et al., 1999) and found coincident immunoreactivity between T $\beta$ R2 and TAG1 (Figures 1E and 1F).

### TGF- $\beta$ Signaling is Required for Axon Development *In Vivo*

Long-term fluorescence imaging studies of newborn neurons in the VZ have shown that axon specification occurs soon after terminal cell division and axon extension occurs during migration (Hatanaka and Murakami, 2002; Noctor et al., 2004). Intriguingly, expression of TGF- $\beta$ 2 ligand (and to a lesser extent TGF- $\beta$ 3) is highly restricted to the VZ and SVZ of embryonic neocortex (Figure S1), precisely the location of axon initiation (Hatanaka and Murakami, 2002; Noctor et al., 2004). To visualize the effect of TGF- $\beta$  signaling in newborn neurons, E14.5 mouse embryos harboring homozygous “floxed” alleles of *Tgfr2* encoding T $\beta$ R2 (*Tgfr2<sup>flox/flox</sup>*) were subjected to intracranial electroporation to introduce a bicistronic plasmid encoding GFP and Cre recombinase selectively into neuronal precursors in the VZ (Barnes et al., 2007; Chytil et al., 2002; Hand et al., 2005; Saito and Nakatsuji, 2001). Following electroporation, embryos were placed back into the mother and allowed to develop for an additional five days (E19.5), at which point the morphogenesis of GFP-positive migrating neurons examined. Immunocytochemical labeling after electroporation revealed that newborn neurons expressing GFP (and thus Cre) lacked detectable expression of T $\beta$ R2 (Figure S2A), indicating effective conditional ablation of *Tgfr2*. In *Tgfr2<sup>flox/flox</sup>* littermate controls electroporated with GFP alone, GFP-positive neurons progressively traveled through the IZ and terminated their migration at the CP, where they began to elaborate dendritic processes (Figures 2A and 2C). Most migrating neurons possessed stereotypical bipolar morphologies consisting of a leading process and a long trailing edge axon (Figures 2A and 2C). In contrast, cells expressing Cre, and thus lacking T $\beta$ R2, failed to form axons despite the extension of a leading edge process (Figures 2B and 2C). Moreover, whereas bundles of GFP-positive axons coursing through the IZ were observed in control animals, such structures were not seen in Cre-expressing animals (Figure 2D).

Next, we performed *ex vivo* electroporation and organotypic slice culture in *Tgfr2<sup>flox/flox</sup>* animals for detailed analysis of neuronal morphogenesis. Labeled neurons from E14.5 embryos was followed over the course of five days in slice culture, during which time they polarize and migrate to the CP in a manner highly similar to events *in vivo* (Figure 2E) (Barnes et al.,

2007; Hand et al., 2005). Similar to our *in utero* experiments, we found that control neurons expressing GFP alone possessed stereotypical bipolar morphologies (Figure 2F and 2H) whereas Cre-expressing neurons lacking T $\beta$ R2 failed to form a distinguishable axon (Figure 2G and 2H). Indeed,  $82.3 \pm 6.4\%$  of control neurons possessed a morphologically discernable axon compared to  $30.2 \pm 8.4\%$  of *Tgfr2* null cells (T $\beta$ R2-KO) (Figure 2I). Moreover, whereas  $84.1 \pm 6.5\%$  of WT cells in the CP and  $81.2 \pm 4.8\%$  of cells in the IZ possessed axons, only  $32.5 \pm 6.3\%$  of T $\beta$ R2-KO cells in the CP and  $30.1 \pm 8.4\%$  in the IZ had discernable axons (Figure S2C), suggesting that this effect was consistent regardless of the migrational state, and hence the age, of the neuron.

In addition to defects in axon formation, T $\beta$ R2-KO neurons exhibited impaired migration to the cortical plate. In neocortex from *Tgfr2<sup>lox/lox</sup>* mice transfected with GFP, GFP-positive neurons migrated to the IZ and CP (Figures 2A, 2F, and S2D; Movie S1). However, many T $\beta$ R2-KO neurons expressing Cre were present within deep cortical layers and failed to migrate (Figures 2B, 2G, and S2D; Movie S1). Whereas a large population of WT cells was found in the CP five days after electroporation (% of labeled cells: VZ/SVZ,  $4.1 \pm 1.4$ ; IZ,  $51.4 \pm 4.4$ ; CP,  $45.5 \pm 1.5$ ; Figure S2D), T $\beta$ R2-KO cells were more abundant in the IZ (% of labeled cells: VZ/SVZ,  $8.4 \pm 1.0$ ; IZ,  $78.8 \pm 5.0$ ; CP,  $12.7 \pm 6.7$ ; Figure S2D). Cells within this deep layer were immunonegative for nestin (Figure S2B), indicating that TGF- $\beta$  signaling affects migration, but not differentiation from radial glial precursors.

In time-lapse imaging experiments, we observed that neurons from *Tgfr2<sup>lox/lox</sup>* mice transfected with GFP alone migrated normally through the IZ and elaborated a dynamic leading edge and a trailing edge axon (Figure 2J and Movie S1). Similar to WT neurons, T $\beta$ R2-KO neurons possessed highly dynamic leading edge processes that extended, retracted, and branched over the 20 hour imaging period (Figure 2K and Movie S1). However, these cells had impaired cell body translocation and failed to exhibit axonal growth at their trailing edge (Figure 2K and Movie S1). Together, these findings demonstrate an obligatory role for TGF- $\beta$  signaling in neuronal polarity and axon specification in developing neocortex.

### TGF- $\beta$ Receptor Distribution is Polarized during Neuronal Development

As loss of T $\beta$ R2 prevents axon but not dendrite formation (Figure 2), we tested whether the axon-specific effect of TGF- $\beta$  signaling results from subcellular confinement of receptor distribution. We first examined immature E14.5 neurons exiting the SVZ of the lateral ventricle and found that T $\beta$ R2 immunoreactivity is concentrated within trailing edge processes (Figures 3A), which become the axon (Noctor et al., 2004). Quantification of T $\beta$ R2 immunoreactivity in these cells revealed that T $\beta$ R2 expression is elevated throughout trailing-edge axons but not in leading edge processes (Figure 3B). Moreover, T $\beta$ R2 expression was higher within the proximal axon compared to the distal axon (Figure 3C).

To elaborate further on this observation, we cultured neurons from E18 rat hippocampi and visualized the surface distribution of T $\beta$ R1 and T $\beta$ R2 during axon specification by immunolabeling (Figure S3). In stage 2 neurons lacking axons (DIV 2), T $\beta$ R1 and T $\beta$ R2 were diffusely distributed over the cell surface with a few receptor clusters evident as discrete foci at the tips of all neurites (Figures 3D, top panels; and 3E). However, by stage 3 (DIV 4), T $\beta$ R1 and T $\beta$ R2 were enriched within the axon and largely absent from dendrites (Figure 3D, bottom panels; and 3F). TGF- $\beta$  receptors were abundant in axonal shafts and in growth cones as diffuse surface staining and discrete puncta, but were largely absent from dendritic growth cones (Figures 3D, bottom panels; 3E and 3F). Quantitative analysis revealed that distal axons had  $54.5 \pm 0.1\%$  more T $\beta$ R1 and  $72.3 \pm 0.1\%$  more T $\beta$ R2 than distal dendrites on the same neurons (Figure 3G).

## Axon Specification by TGF- $\beta$ Signaling is Cell Autonomous

To analyze neuronal differentiation and morphogenesis in the absence of TGF- $\beta$  signaling in more detail, we performed *ex vivo* electroporation of neuronal progenitors at E14.5 and then dissociated and cultured the cells to assess axon development after five days in culture. Most control neurons transfected with GFP extended multiple MAP-2 positive dendrites and a single, long tau-1 positive, MAP-2 negative axon (Figure S4A, top panels). Neurons lacking T $\beta$ R2 also possessed multiple MAP-2 positive dendrites suggesting that neuronal differentiation is not affected in these cells, but they failed to elaborate a tau-1 positive axon (Figure S4A, bottom panels). Indeed, whereas  $77.4 \pm 0.6\%$  of controls cells had a single axon, only  $37.3 \pm 1.8\%$  of T $\beta$ R2-KO neurons elaborated an axon (Figure S4B), indicating that TGF- $\beta$  signaling is required for axon initiation *in vitro*.

As embryonic cortical electroporation initially labels nestin-positive radial glial progenitors in the ventricular zone (VZ) (Hand et al., 2005), we could not determine whether the loss of axons in T $\beta$ R2-KO neurons occurs after or immediately prior to the terminal cell division of neuronal progenitor cells. To address this issue, we utilized dissociated E18 rat hippocampal neuronal cultures, which consist of terminally differentiated postmitotic neurons (Banker and Cowan, 1977). In an initial set of experiments, we treated freshly plated neurons with SB-431542, a potent and selective small molecule inhibitor of T $\beta$ R1. Whereas a large majority of control cells treated with DMSO alone possessed a single axon ( $80.3 \pm 2.1\%$ , Figure S4C and S4E), cells grown in the presence of SB-431542 for 72 hours lacked a distinguishable axon ( $22.9 \pm 3.4\%$ , Figure S4D and S4E). Next, we disrupted TGF- $\beta$  signaling in individual neurons by sparsely transfecting cultures with a kinase-inactive mutant form of T $\beta$ R2 (K277R, hereafter referred to as KR) (Wrana et al., 1992) along with GFP. After 65-72 hours of growth, cells expressing GFP alone possessed a single long tau-1 positive axon (Figures 4A and 4B, top panels), but cells expressing T $\beta$ R2-KR possessed multiple short neurites of roughly equivalent length that lacked tau-1 immunoreactivity (Figures 4A and 4B, bottom panels). Neurons expressing T $\beta$ R2-KR often produced thin, filopodia-like extensions that suggested disorganization in cytoskeletal arrangement (Figure 4B, bottom panels). When quantified, the longest neurite in T $\beta$ R2-KR expressing cells was on average  $167 \mu\text{m}$  shorter than axons of control cells (T $\beta$ R2-KR,  $138 \pm 45 \mu\text{m}$ ; GFP,  $305 \pm 14 \mu\text{m}$ ) (Figure 4C). Moreover, whereas most control neurons expressing GFP possessed a single tau-1 positive axon by 72 hours ( $84.5\% \pm 4.4\%$  with one axon; Figure 4D), most cells expressing T $\beta$ R2-KR lacked a tau-1 positive axon ( $60.8 \pm 5.3\%$  with no axon; Figure 4D).

To test whether TGF- $\beta$  signaling is sufficient to specify axons, we enhanced TGF- $\beta$  signaling by expressing the constitutively active wild-type (WT) form of T $\beta$ R2. After 65-72 hours, cells transfected with GFP possessed long single axons whereas cells with increased TGF- $\beta$  signaling generated multiple tau-1-positive and MAP-2-negative axons (Figures 4E and 4F). When quantified,  $46.2 \pm 4.9\%$  of T $\beta$ R2-WT expressing cells possessed supernumerary axons compared to  $3.2 \pm 2.9\%$  in GFP expressing cells (Figure 4G). Moreover, to test whether augmented TGF- $\beta$  signaling could induce axons after polarity establishment, we expressed T $\beta$ R2-WT in fully polarized DIV5 neurons. When analyzed two days later (DIV7), nearly half of T $\beta$ R2-WT expressing cells elaborated multiple long tau-1 positive axons ( $49.0 \pm 2.8\%$ ,  $n = 43$ ; Figures S4F and S4G), a phenotype seldom observed for control cells ( $3.3 \pm 2.7\%$  neurons with  $\geq 2$  axon,  $n = 38$ ; Figure S4F and S4G).

## Exogenous TGF- $\beta$ is Sufficient to Spatially Direct Neurite Outgrowth and Axon Specification

To address whether local TGF- $\beta$  signaling drives axon specification, we used TGF- $\beta$ -conjugated polystyrene beads to examine cellular responses upon bead contact. Strikingly, when TGF- $\beta$  beads were placed in contact with single neurites of unpolarized neurons, we observed rapid growth of the contacted neurite characteristic of the rapid outgrowth that occurs

during axon specification *in vitro* (Figures 5A and 5B, Movie S2) (Dotti et al., 1988). Stimulated neurites doubled in length over the course an hour while the lengths of unstimulated neurites remained unchanged (Figure 5C). The observed effect of local TGF- $\beta$  was not due to mechanical contact as polystyrene beads conjugated with bovine serum albumin (BSA) had no effect on neurite growth (Figure 5D). Moreover, there was no difference in the initial lengths of stimulated ( $27.3 \pm 3.4 \mu\text{m}$ ) and unstimulated neurites ( $28.4 \pm 2.5 \mu\text{m}$ ) indicating that there was no selection bias for long neurites already primed to become an axon.

To examine whether rapid neurite outgrowth induced by local TGF- $\beta$  coincides with molecular differentiation of an axon, we cultured hippocampal neurons on coverslips with a striped pattern of TGF- $\beta$  substrate (Walter et al., 1987)(see Supplemental Experimental Procedures for details). After 72 hours, neurons were fixed and dendrites and axons visualized by MAP-2 and tau-1 immunoreactivity, respectively. In cases where neurons adhered near the border of a TGF- $\beta$  stripe, the nascent axon invariably arose from the neurite that contacted the stripe and the tau-1 positive axon projected into the stripe (Figure 5E, top panels). Interestingly, neurons seeded directly on a TGF- $\beta$  stripe formed multiple tau-1 positive axons (Figure 5E, bottom panels). Indeed, when cells were grown on a contiguous substrate of TGF- $\beta$ ,  $23.7 \pm 4.8\%$  of cells possessed multiple axons compared to  $4.5 \pm 1.0\%$  of cells grown on laminin (Figure S5).

To quantify the effect of local TGF- $\beta$  on axon induction, we compared the directional projection of axons on a cell-by-cell basis using tau-1 immunoreactivity. We divided the uncoated area between the coated stripes into  $45 \mu\text{m}$  halves, and cells with somas completely contained in either half were imaged for analysis. Camera lucida traces of tau-1 images were overlaid onto a grid as a compilation such that cells projecting axons towards the closest stripe were oriented upwards and projections away from the stripe were oriented downwards on the grid (Figure 5F). Using this method, we found that  $85.7 \pm 7.3\%$  of neurons had axons that arose from neurites which contacted zones of TGF- $\beta$  (Figure 5G). On the other hand, axons were randomly directed in cells grown on striped coverslips containing BSA alone (Figure 5H).

### TGF- $\beta$ Signaling is Mediated by Par6 Phosphorylation

In epithelial cells, TGF- $\beta$  receptor activity is localized to tight junctions within the plasma membrane through an interaction between T $\beta$ R1 and Par6, a member of the conserved Par3/Par6/PKC $\zeta$  polarity complex (Hung and Kemphues, 1999) and a key mediator of axon specification (Shi et al., 2003). We thus hypothesized that TGF- $\beta$  signaling may induce axon formation *in vivo* by directly coupling to Par6. We simultaneously labeled brain slices from E18 mouse embryos with antibodies against Par6 and T $\beta$ R1 and found that both are enriched within apical domains of radial glia in the VZ (Figures 6A and 6B). In dissociated hippocampal neurons, surface T $\beta$ R1 and Par6 colocalize in discrete punctate clusters within growth cones of undifferentiated neurites (Figure 6C), particularly within filopodial protrusions (Figure 6D). Further, both Par6 and Par3 co-immunoprecipitated with T $\beta$ R1 from E18 rat forebrain lysates (Figure 6E), indicating that T $\beta$ R1 and Par3/Par6 form a biochemical complex in developing brain.

After ligand stimulation, T $\beta$ R2 phosphorylates Par6 at serine 345 (S345), leading to the local recruitment of the ubiquitin ligase Smurf1 and subsequent degradation of RhoA (Ozdamar et al., 2005). We generated Par6 mutants to prevent (S345A) or mimic (S345E) phosphorylation at serine 345. Whereas neurons expressing GFP produced long, single axons, cells expressing Par6-S345A lacked axons (Figures 6F and 6G) similar to the effect observed upon inhibition of TGF- $\beta$  receptor signaling (Figures 4, S4, and S5). In contrast, neurons expressing Par6-S345E formed axons (Figures 6F and 6G) and coexpression of Par6-S345A with T $\beta$ R2-WT prevented the gain of function of T $\beta$ R2-WT overexpression (Figure S6), indicating that the effect of Par6-S345A was not a nonselective effect of overexpressing Par6 and showing that Par6 phosphorylation is required downstream of TGF- $\beta$  receptor signaling.

## TGF- $\beta$ Signaling Mediates Axon Formation *in Vivo* through Site-Specific Phosphorylation of Par6

To address whether Par6 phosphorylation by TGF- $\beta$  receptors determines neuronal polarity *in vivo*, we examined axon initiation and migration of neocortical neurons expressing either Par6-S345A or Par6-S345E. Canonical TGF- $\beta$  signaling was genetically ablated in neocortical progenitors by intracranial electroporation of Cre in E15 *Tgfb $\beta$ 2<sup>lox/lox</sup>* mice and Par6 constructs were co-expressed along with Cre. Neocortical slices were then prepared and cultured for five days to allow for neuronal migration and polarization to proceed (Figure 2E; see Experimental Procedures for details). T $\beta$ R2-KO neurons expressing Par6-S345A were similar in morphology to T $\beta$ R2-KO neurons and failed to initiate axon growth (Figures 7A and 7C, see also Figure 2). In contrast, T $\beta$ R2-KO neurons expressing Par6-S345E reliably produced axons (Figures 7B and 7D), suggesting that site-specific phosphorylation of Par6 rescues axon specification in the absence of TGF- $\beta$  receptor signaling. Quantitative analysis revealed that T $\beta$ R2-KO neurons expressing Par6-S345E possessed axons at nearly the same frequency as WT neurons ( $70.3 \pm 6.8\%$  with axons, compared to  $85.2 \pm 6.2\%$  for WT neurons expressing GFP; Figures 7E and 2I). On the other hand, Par6-S345A failed to rescue axon formation in T $\beta$ R2 KO neurons ( $36.6 \pm 9.2\%$  of cells with axons compared to  $31.6 \pm 7.2\%$  for T $\beta$ R2-KO alone; Figures 7E and 2I). Although expression of Par6-S345E rescued axonal defects, it had no effect on migration (Figure 7F), indicating that Par6 phosphorylation is selectively required for axon specification in developing pyramidal neurons. Indeed, only  $18.6 \pm 1.9\%$  of T $\beta$ R2-KO cells expressing Par6-S345A and  $15.3 \pm 1.4\%$  of cells expressing Par6-S345E migrated to the CP after 5 DIV (Figure 7F), which were comparable to numbers seen for T $\beta$ R2-KO cells expressing GFP alone (Figure S2D). Together, these results demonstrate that axon formation *in vivo* requires TGF- $\beta$  signaling via site-specific phosphorylation of Par6.

## Discussion

### An Extrinsic Signal for Axon Specification

Despite an extensive and increasing understanding of intracellular mechanisms underlying axon specification (Barnes and Polleux, 2009), the extrinsic cues that direct neuronal polarity *in vivo* have been obscure and controversial. Previous work has shown that many external manipulations can trigger axon formation and growth in dissociated cultures (Barnes and Polleux, 2009). However, whether such factors play a role in neuronal polarity *in vivo* has remained unclear since knockout mice lacking these signaling molecules or their receptors show no defect in axon formation (Chen et al., 2008; Ernfors et al., 1994; Jones et al., 1994; Kappeler et al., 2008; Liu et al., 1993; Vicario-Abejon et al., 2004).

Our findings strongly suggest that TGF- $\beta$  is the dominant extracellular signaling molecule required for axon specification in the developing brain. However, we cannot rule out that TGF- $\beta$  signaling may work in concert or be modified by other extracellular factors in neurons. In this regard, it is interesting to note that signaling by extracellular molecules such as BMPs (Schermer et al., 2007), BDNF (Sometani et al., 2001), Wnt (Falk et al., 2008; Narimatsu et al., 2009), sonic hedgehog (Li et al., 2008), FGF (Song et al., 2002), NGF (Saad et al., 1991), and semaphorins (Ikegami et al., 2004) can influence TGF- $\beta$  signaling. Moreover, many of these molecules have been demonstrated to be axon guidance molecules during neural development (Charron and Tessier-Lavigne, 2005), suggesting that a complex synergistic network of extracellular factors mediate the initial stages of axon formation.

Interestingly, we found that expression of Par6-S345E results in the formation of a single axon, despite diffuse expression throughout the cell (Figure 6F and G; Figure 7B – E). This observation suggests the presence of a strong repressive mechanism that prevents the formation of supernumerary axons within a single cell. Indeed, recent work has demonstrated differential

regulation of cAMP and cGMP in the axon and dendrites, suggesting a mechanistic basis for distinct pro and anti-axon signals during the initial stages of neuronal polarization (Shelly et al., 2010). Whether such a response is cell-intrinsic or directed by additional extracellular cues remains to be clarified.

### TGF- $\beta$ in Brain Development

The expression pattern of TGF- $\beta$ 2, and to a lesser extent TGF- $\beta$ 3 (Figure S1B and C) coincides with the anatomical orientation of neocortical axons since principal neurons arising from the lateral ventricle all project their axons toward the ventricular zone. Thus, newborn neurons in the ventricular zone will be exposed to a gradient of TGF- $\beta$ 2 ligand with highest levels present near the ventricular surface, thereby giving a uniform vector to axon specification (Figure 7G).

The autocrine nature of TGF- $\beta$  signaling has been well studied for its role in cell transformation and metastatic growth (Sporn and Todaro, 1980), and such a mechanism may provide a polarity feedback loop to ensure prolonged axon development. After an initial external polarizing cue, local TGF- $\beta$  receptor signaling coupled with Par3/Par6 complex accumulation and further polarized TGF- $\beta$  secretion may facilitate the local accumulation and feedback stabilization of polarity-generating molecules for axon specification.

### Axon Specification Through Extracellular Control of the Par3/Par6 Complex

Here we have shown that TGF- $\beta$  signaling for neuronal polarity depends on phosphorylation of Par6 – a multimodular protein that contains a Cdc42-Rac1 interaction-binding (CRIB) motif that allows Par6 to direct Cdc42/Rac1 activity (Joberty et al., 2000). In the presence of TGF- $\beta$  Par6 phosphorylation by T $\beta$ R2 recruits the ubiquitin ligase Smurf1, which in turn promotes the proteasomal degradation of RhoA (Ozdamar et al., 2005). In this manner, the local stoichiometry of Rho GTPases can be modified at the site of TGF- $\beta$  signaling to alter local actin organization, a well-documented hallmark of axon specification (Bradke and Dotti, 1999).

The TGF- $\beta$  signaling pathway described in this work plays an important role in epithelial-mesenchymal transition (EMT), a well-established program of epithelial morphological plasticity characterized by the loss of cell-cell contacts and independent cell migration (Greenburg and Hay, 1982; Ozdamar et al., 2005). Intriguingly, many aspects of nervous system development are similar to EMT. For example, radial glia possess architecture similar to epithelial cells with small, ventricularly-oriented apical endfeet and pia-oriented basolateral domains separated by cell-cell junctions (Rakic, 2003). Thus, we propose that neuronal morphogenesis may have coopted signaling mechanisms analogous to EMT, in which the loss of epithelial polarity, remodeling of cell-cell and cell-matrix adhesion contacts, and reorganization of the actin cytoskeleton precede morphological differentiation (Zavadil and Bottinger, 2005). How TGF- $\beta$  functions to coordinate these various events in early neuronal morphogenesis will be a fertile area for future research.

## Experimental Procedures

### Animals

All animals were used according to protocols approved by the Institutional Animal Care and Use Committee of the Duke University Medical Center, the University of North Carolina, and in accordance with NIH guidelines. Noon following breeding was considered to be E0.5. *Tgfr2<sup>flox/flox</sup>* mice were obtained from the Mouse Models for Human Cancers Consortium (MMHCC) repository at the National Cancer Institute. Timed pregnant rats were obtained from Charles River Laboratories.



## Electroporation, Slice and Dissociated Cell Cultures

For our *in utero* experiment, *E14.5* mice were anesthetized using 2.5% 2,2,2-tribromoethanol and a small 1-2 cm incision was made along the midline to access the uterus. The lateral ventricles of the embryos were injected with 2 µg/µl of plasmid in 1x PBS with 0.1% Fast Green dye for visualization. The embryos were electroporated using four pulses of 50V for 50 ms with a 500 ms interval. Afterwards, the uterus was placed back in the abdominal cavity and the incision was sutured. Mice were allowed to recover and embryos were collected at E19.5. All surgeries strictly adhered to IACUC approved protocols.

For *ex vivo* slice cultures, dorsal telencephalic progenitors were labeled by injecting pCIG2 plasmid DNA (0.5 µg/µl) or pCIG2-Cre plasmid DNA (0.5 µg/µl) diluted in a 0.1% Fast Green solution into the lateral ventricles of decapitated E14.5 *Tgbr2<sup>flox/flox</sup>* mouse heads using a Picospritzer II (General Valve). Electric potentials were generated across intact heads using gold-coated electrodes attached to an ECM 830 electroporator using four 100 ms 45V pulses separated by 100 ms intervals. Immediately after electroporation, brains were dissected, Vibratome sectioned at 250 µm, and maintained as organotypic cultures prior to fixation and immunohistochemical labeling as described in the Supplemental Experimental Procedures. Cortical migration analysis was conducted based on previously published methods (Hand et al., 2005). Cortical slices were divided into three zones based on the distance from the lateral ventricle (ventricular zone/sub-ventricular zone, VZ/SVZ; intermediate zone, IZ; cortical plate, CP).

Dissociated rat hippocampal neurons were prepared as described (Ehlers, 2000). Alternatively, primary E14.5 mouse cortical cultures were prepared using a papain-based enzymatic dissociation method as previously described (Polleux and Ghosh, 2002).

## Fluorescence Microscopy and Immunohistochemistry

The imaging methods used in this study are described in detail in the Supplemental Experimental Materials. All data are presented as the mean ± standard error.

## Immobilized TGF-β Bead Assay

Purified recombinant TGF-β1,2,3 (R&D Systems) or BSA was biotinylated using the EZ-link Sulfo-NHS-LC-LC reagent (Pierce) according to the manufacturer's instructions and incubated with streptavidin-conjugated polystyrene beads (Pierce). See Supplemental Experimental Materials for details.

## Substrate Patterning

Glass coverslips with a diameter of 18 mm were coated overnight with poly-D-lysine (1 mg/ml) at 37°C. The next day, coated coverslips were washed three times in sterile water and dried. A silicon matrix (J. Jung, Tuebingen, Germany) consisting of 90 µm channels separated by 90 µm intervals was placed over the coverslip. Channels were filled with a 0.1% solution of Alexa 568-conjugated BSA (Invitrogen) with or without 100 ng/ml TGF-β1, 2, 3 and incubated for 2 h at 37°C. Coverslips were washed prior to cell plating.

## Supplementary Material

Refer to Web version on PubMed Central for supplementary material.

## Acknowledgments

We thank Irina Lebedeva and Marguerita Klein for excellent technical assistance, and Ben Arenkiel, Ian Davison, Juliet Hernandez, Matt Kennedy, and Fan Wang for helpful discussion and critical review of the manuscript. We thank

Irwin Liu and Xiao-Fan Wang for the Tgfr1 shRNA constructs. This work was supported by grants from the NIMH and NINDS to M.D.E. and a Ruth K. Broad Biomedical Foundation fellowship to J.J.Y. M.D.E. is an Investigator of the Howard Hughes Medical Institute.

## References

- Baas AF, Kuipers J, van der Wel NN, Battle E, Koerten HK, Peters PJ, Clevers HC. Complete polarization of single intestinal epithelial cells upon activation of LKB1 by STRAD. *Cell* 2004;116:457–466. [PubMed: 15016379]
- Banker GA, Cowan WM. Rat hippocampal neurons in dispersed cell culture. *Brain Res* 1977;126:397–342. [PubMed: 861729]
- Barnes A, Polleux F. Establishment of axon-dendrite polarity in developing neurons. *Annu Rev Neurosci* 2009;32:347–381. [PubMed: 19400726]
- Barnes AP, Lilley BN, Pan YA, Plummer LJ, Powell AW, Raines AN, Sanes JR, Polleux F. LKB1 and SAD kinases define a pathway required for the polarization of cortical neurons. *Cell* 2007;129:549–563. [PubMed: 17482548]
- Bradke F, Dotti CG. The role of local actin instability in axon formation. *Science* 1999;283:1931–1934. [PubMed: 10082468]
- Charron F, Tessier-Lavigne M. Novel brain wiring functions for classical morphogens: a role as graded positional cues in axon guidance. *Development* 2005;132:2251–2262. [PubMed: 15857918]
- Chen ZL, Haegeli V, Yu H, Strickland S. Cortical deficiency of laminin gamma1 impairs the AKT/GSK-3beta signaling pathway and leads to defects in neurite outgrowth and neuronal migration. *Dev Biol*. 2008
- Chytil A, Magnuson MA, Wright CV, Moses HL. Conditional inactivation of the TGF-beta type II receptor using Cre:Lox. *Genesis* 2002;32:73–75. [PubMed: 11857781]
- Craig AM, Banker G. Neuronal polarity. *Annu Rev Neurosci* 1994;17:267–310. [PubMed: 8210176]
- Dotti CG, Sullivan CA, Banker GA. The establishment of polarity by hippocampal neurons in culture. *J Neurosci* 1988;8:1454–1468. [PubMed: 3282038]
- Ehlers MD. Reinsertion or degradation of AMPA receptors determined by activity-dependent endocytic sorting. *Neuron* 2000;28:511–525. [PubMed: 11144360]
- Ernfors P, Lee KF, Jaenisch R. Mice lacking brain-derived neurotrophic factor develop with sensory deficits. *Nature* 1994;368:147–150. [PubMed: 8139657]
- Falk S, Wurdak H, Ittner LM, Ille F, Sumara G, Schmid MT, Draganova K, Lang KS, Paratore C, Leveen P, et al. Brain area-specific effect of TGF-beta signaling on Wnt-dependent neural stem cell expansion. *Cell Stem Cell* 2008;2:472–483. [PubMed: 18462697]
- Greenburg G, Hay ED. Epithelia suspended in collagen gels can lose polarity and express characteristics of migrating mesenchymal cells. *J Cell Biol* 1982;95:333–339. [PubMed: 7142291]
- Gripp KW, Wotton D, Edwards MC, Roessler E, Ades L, Meinecke P, Richieri-Costa A, Zackai EH, Massague J, Muenke M, et al. Mutations in TGIF cause holoprosencephaly and link NODAL signalling to human neural axis determination. *Nat Genet* 2000;25:205–208. [PubMed: 10835638]
- Hand R, Bortone D, Mattar P, Nguyen L, Heng JI, Guerrier S, Boutt E, Peters E, Barnes AP, Parras C, et al. Phosphorylation of Neurogenin2 specifies the migration properties and the dendritic morphology of pyramidal neurons in the neocortex. *Neuron* 2005;48:45–62. [PubMed: 16202708]
- Hatanaka Y, Murakami F. In vitro analysis of the origin, migratory behavior, and maturation of cortical pyramidal cells. *J Comp Neurol* 2002;454:1–14. [PubMed: 12410614]
- Heine U, Munoz EF, Flanders KC, Ellingsworth LR, Lam HY, Thompson NL, Roberts AB, Sporn MB. Role of transforming growth factor-beta in the development of the mouse embryo. *J Cell Biol* 1987;105:2861–2876. [PubMed: 3320058]
- Hung TJ, Kempnues KJ. PAR-6 is a conserved PDZ domain-containing protein that colocalizes with PAR-3 in *Caenorhabditis elegans* embryos. *Development* 1999;126:127–135. [PubMed: 9834192]
- Ikegami R, Zheng H, Ong SH, Culotti J. Integration of semaphorin-2A/MAB-20, ephrin-4, and UNC-129 TGF-beta signaling pathways regulates sorting of distinct sensory rays in *C. elegans*. *Dev Cell* 2004;6:383–395. [PubMed: 15030761]

- Ishihara A, Saito H, Abe K. Transforming growth factor-beta 1 and -beta 2 promote neurite sprouting and elongation of cultured rat hippocampal neurons. *Brain Res* 1994;639:21–25. [PubMed: 8180834]
- Joberty G, Petersen C, Gao L, Macara IG. The cell-polarity protein Par6 links Par3 and atypical protein kinase C to Cdc42. *Nat Cell Biol* 2000;2:531–539. [PubMed: 10934474]
- Jones KR, Farinas I, Backus C, Reichardt LF. Targeted disruption of the BDNF gene perturbs brain and sensory neuron development but not motor neuron development. *Cell* 1994;76:989–999. [PubMed: 8137432]
- Kappeler L, De Magalhaes Filho CM, Dupont J, Leneuve P, Cervera P, Perin L, Loudes C, Blaise A, Klein R, Epelbaum J, et al. Brain IGF-1 receptors control mammalian growth and lifespan through a neuroendocrine mechanism. *PLoS Biol* 2008;6:e254. [PubMed: 18959478]
- Kawano H, Fukuda T, Kubo K, Horie M, Uyemura K, Takeuchi K, Osumi N, Eto K, Kawamura K. Pax-6 is required for thalamocortical pathway formation in fetal rats. *J Comp Neurol* 1999;408:147–160. [PubMed: 10333267]
- Klein R, Smeyne RJ, Wurst W, Long LK, Auerbach BA, Joyner AL, Barbacid M. Targeted disruption of the *trkB* neurotrophin receptor gene results in nervous system lesions and neonatal death. *Cell* 1993;75:113–122. [PubMed: 8402890]
- Kriegstein AR, Noctor SC. Patterns of neuronal migration in the embryonic cortex. *Trends Neurosci* 2004;27:392–399. [PubMed: 15219738]
- Li M, Li C, Liu YH, Xing Y, Hu L, Borok Z, Kwong KY, Minoo P. Mesodermal deletion of transforming growth factor-beta receptor II disrupts lung epithelial morphogenesis: cross-talk between TGF-beta and Sonic hedgehog pathways. *J Biol Chem* 2008;283:36257–36264. [PubMed: 18990706]
- Liu JP, Baker J, Perkins AS, Robertson EJ, Efstratiadis A. Mice carrying null mutations of the genes encoding insulin-like growth factor I (*Igf-1*) and type 1 IGF receptor (*Igf1r*). *Cell* 1993;75:59–72. [PubMed: 8402901]
- Loeys BL, Chen J, Neptune ER, Judge DP, Podowski M, Holm T, Meyers J, Leitch CC, Katsanis N, Sharifi N, et al. A syndrome of altered cardiovascular, craniofacial, neurocognitive and skeletal development caused by mutations in *TGFBR1* or *TGFBR2*. *Nat Genet* 2005;37:275–281. [PubMed: 15731757]
- Mecha M, Rabadan MA, Pena-Melian A, Valencia M, Mondejar T, Blanco MJ. Expression of TGF-betas in the embryonic nervous system: analysis of interbalance between isoforms. *Dev Dyn* 2008;237:1709–1717. [PubMed: 18498095]
- Murphy SJ, Dore JJ, Edens M, Coffey RJ, Barnard JA, Mitchell H, Wilkes M, Leof EB. Differential trafficking of transforming growth factor-beta receptors and ligand in polarized epithelial cells. *Mol Biol Cell* 2004;15:2853–2862. [PubMed: 15075369]
- Narimatsu M, Bose R, Pye M, Zhang L, Miller B, Ching P, Sakuma R, Luga V, Roncari L, Attisano L, et al. Regulation of planar cell polarity by Smurf ubiquitin ligases. *Cell* 2009;137:295–307. [PubMed: 19379695]
- Ng J. TGF-beta signals regulate axonal development through distinct Smad-independent mechanisms. *Development* 2008;135:4025–4035. [PubMed: 19004854]
- Noctor SC, Martinez-Cerdeno V, Ivic L, Kriegstein AR. Cortical neurons arise in symmetric and asymmetric division zones and migrate through specific phases. *Nat Neurosci* 2004;7:136–144. [PubMed: 14703572]
- Ozdamar B, Bose R, Barrios-Rodiles M, Wang HR, Zhang Y, Wrana JL. Regulation of the polarity protein Par6 by TGFbeta receptors controls epithelial cell plasticity. *Science* 2005;307:1603–1609. [PubMed: 15761148]
- Polleux F, Dehay C, Kennedy H. The timetable of laminar neurogenesis contributes to the specification of cortical areas in mouse isocortex. *J Comp Neurol* 1997;385:95–116. [PubMed: 9268119]
- Polleux F, Ghosh A. The slice overlay assay: a versatile tool to study the influence of extracellular signals on neuronal development. *Sci STKE* 2002;2002:PL9. [PubMed: 12060788]
- Rakic P. Developmental and evolutionary adaptations of cortical radial glia. *Cereb Cortex* 2003;13:541–549. [PubMed: 12764027]
- Saad B, Constam DB, Ortmann R, Moos M, Fontana A, Schachner M. Astrocyte-derived TGF-beta 2 and NGF differentially regulate neural recognition molecule expression by cultured astrocytes. *J Cell Biol* 1991;115:473–484. [PubMed: 1717486]

- Saito T, Nakatsuji N. Efficient gene transfer into the embryonic mouse brain using in vivo electroporation. *Dev Biol* 2001;240:237–246. [PubMed: 11784059]
- Schnerer O, Meurer SK, Tihaa L, Gressner AM, Weiskirchen R. Endoglin differentially modulates antagonistic transforming growth factor-beta1 and BMP-7 signaling. *J Biol Chem* 2007;282:13934–13943. [PubMed: 17376778]
- Shelly M, Cancedda L, Heilshorn S, Sumbre G, Poo MM. LKB1/STRAD promotes axon initiation during neuronal polarization. *Cell* 2007;129:565–577. [PubMed: 17482549]
- Shelly M, Lim BK, Cancedda L, Heilshorn SC, Gao H, Poo MM. Local and long-range reciprocal regulation of cAMP and cGMP in axon/dendrite formation. *Science* 2010;327:547–552. [PubMed: 20110498]
- Shi SH, Jan LY, Jan YN. Hippocampal neuronal polarity specified by spatially localized mPar3/mPar6 and PI 3-kinase activity. *Cell* 2003;112:63–75. [PubMed: 12526794]
- Shi Y, Massague J. Mechanisms of TGF-beta signaling from cell membrane to the nucleus. *Cell* 2003;113:685–700. [PubMed: 12809600]
- Sometani A, Kataoka H, Nitta A, Fukumitsu H, Nomoto H, Furukawa S. Transforming growth factor-beta1 enhances expression of brain-derived neurotrophic factor and its receptor, TrkB, in neurons cultured from rat cerebral cortex. *J Neurosci Res* 2001;66:369–376. [PubMed: 11746354]
- Song QH, Klepeis VE, Nugent MA, Trinkaus-Randall V. TGF-beta1 regulates TGF-beta1 and FGF-2 mRNA expression during fibroblast wound healing. *Mol Pathol* 2002;55:164–176. [PubMed: 12032227]
- Sosa L, Dupraz S, Laurino L, Bollati F, Bisbal M, Caceres A, Pfenninger KH, Quiroga S. IGF-1 receptor is essential for the establishment of hippocampal neuronal polarity. *Nat Neurosci* 2006;9:993–995. [PubMed: 16845384]
- Sporn MB, Todaro GJ. Autocrine secretion and malignant transformation of cells. *N Engl J Med* 1980;303:878–880. [PubMed: 7412807]
- Tomoda T, Shirasawa T, Yahagi YI, Ishii K, Takagi H, Furiya Y, Arai KI, Mori H, Muramatsu MA. Transforming growth factor-beta is a survival factor for neonate cortical neurons: coincident expression of type I receptors in developing cerebral cortices. *Dev Biol* 1996;179:79–90. [PubMed: 8873755]
- Vicario-Abejon C, Fernandez-Moreno C, Pichel JG, de Pablo F. Mice lacking IGF-I and LIF have motoneuron deficits in brain stem nuclei. *Neuroreport* 2004;15:2769–2772. [PubMed: 15597051]
- Walter J, Kern-Veits B, Huf J, Stolze B, Bonhoeffer F. Recognition of position-specific properties of tectal cell membranes by retinal axons in vitro. *Development* 1987;101:685–696. [PubMed: 3503693]
- Wrana JL, Attisano L, Carcamo J, Zentella A, Doody J, Laiho M, Wang XF, Massague J. TGF beta signals through a heteromeric protein kinase receptor complex. *Cell* 1992;71:1003–1014. [PubMed: 1333888]
- Zavadil J, Bottinger EP. TGF-beta and epithelial-to-mesenchymal transitions. *Oncogene* 2005;24:5764–5774. [PubMed: 16123809]

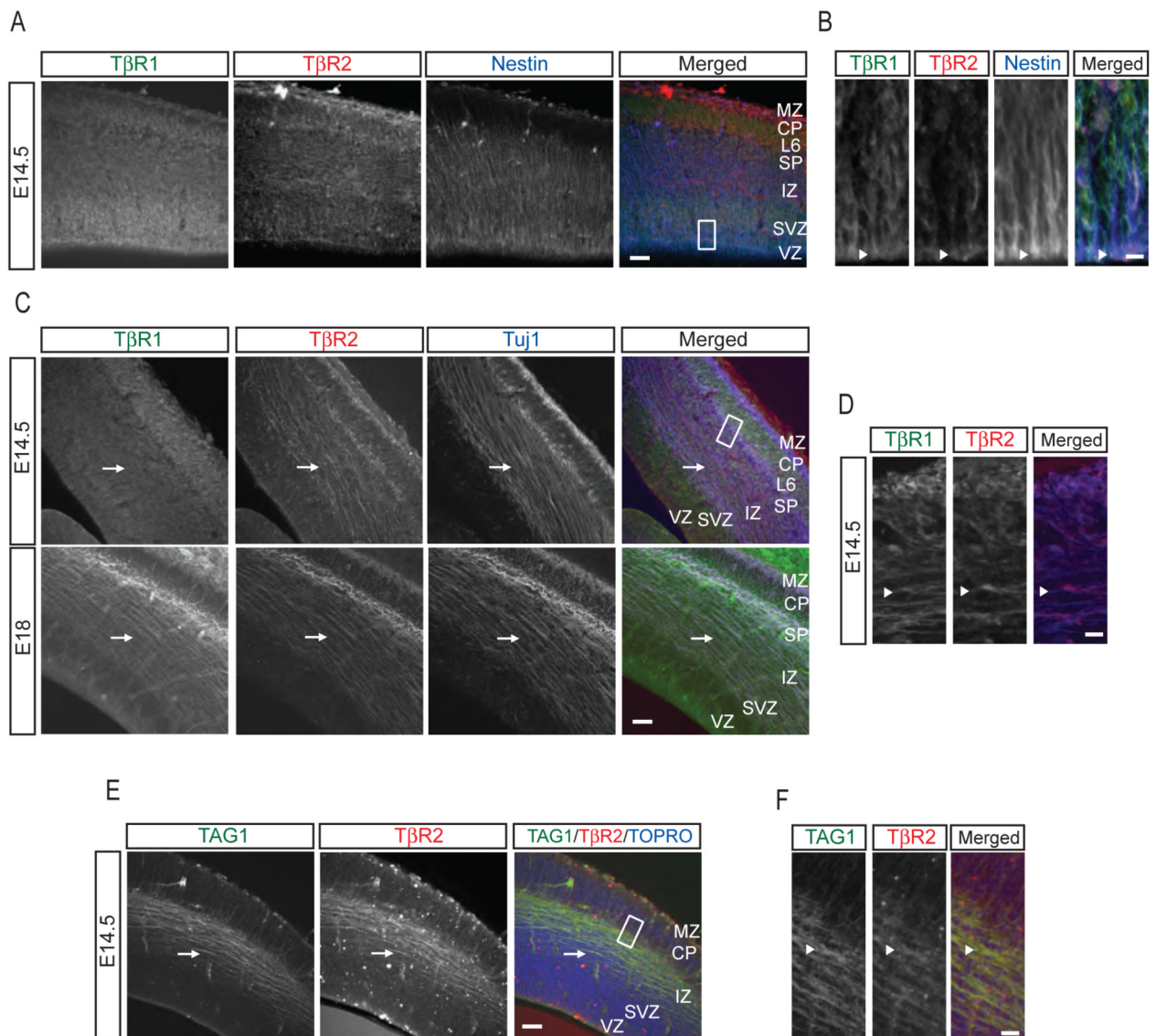


**Figure 1.**

**Axonal Expression of TGF- $\beta$  Receptors in the Developing Mouse Neocortex**

(A) Sections of neocortex from embryonic day 14.5 (E14.5) mouse embryos processed for immunohistochemistry and triple labeled for T $\beta$ R1, T $\beta$ R2, and nestin. Scale bar, 50  $\mu$ m. MZ, marginal zone; CP, cortical plate; L6, layer 6; SP, subcortical plate; IZ, intermediate zone; SVZ, subventricular zone; VZ, ventricular zone.

(B) Magnified panels of area demarcated by white dashed box in (A) showing apical enrichment of TGF- $\beta$  receptors in nestin-positive radial glia (arrowheads). Scale bar, 5  $\mu$ m.

(C) Sections of mouse neocortex at E14.5 (top) or E18 (bottom) labeled for T $\beta$ R1, T $\beta$ R2, and the neuron-specific  $\beta$ -tubulin III marker Tuj1. Arrow shows Tuj1-positive fasciculations in the IZ. Scale bar, 50  $\mu$ m. Abbreviations as in (A).

(D) Magnified panels of area demarcated by white dashed box in (C) showing the presence of TGF- $\beta$  receptors in the IZ at E14.5. Arrowhead indicates an axon positive for both T $\beta$ R1 and T $\beta$ R2. Scale bar, 5  $\mu$ m.

(E) Sections of E14.5 mouse neocortex labeled with the corticofugal axon marker TAG1, T $\beta$ R2, and the nuclear stain TOPRO-3 demonstrating the presence of T $\beta$ R2 in cortical axons (arrows). Scale bar, 50  $\mu$ m.

(F) Magnified panels of area demarcated by white dashed box in (E) showing strong T $\beta$ R2 staining in TAG1-positive axons. Scale bar, 5  $\mu$ m.

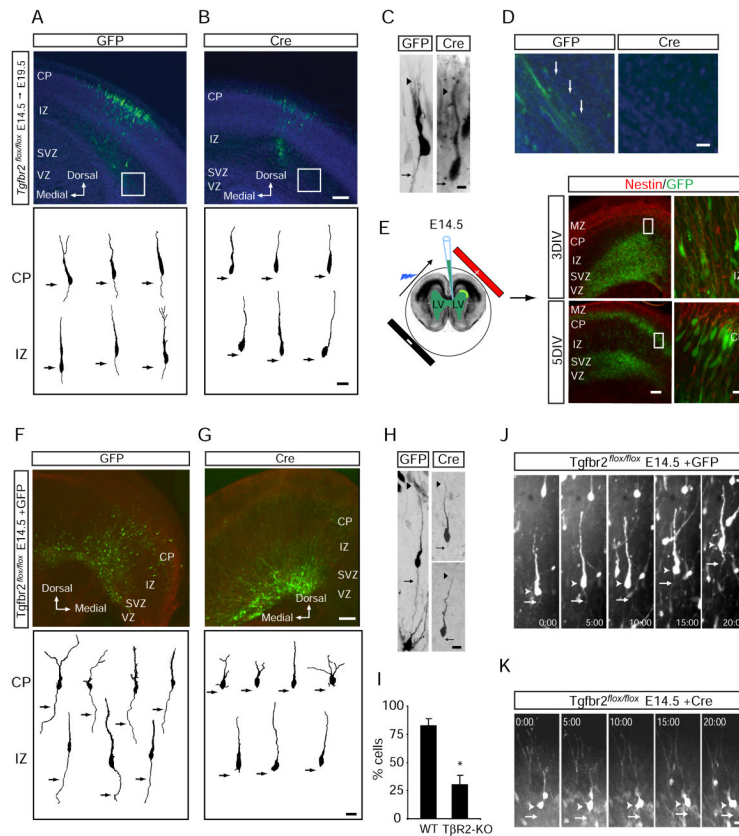


**Figure 2.**

**TGF- $\beta$  Signaling is Required for Neocortical Development *In Vivo***

(A) E19.5 neocortical slice from a *Tgfr2<sup>flox/flox</sup>* embryo electroporated at E14.5 with GFP to label newborn neurons. Top panel shows neuronal migration 5 days after electroporation. Bottom panel contains camera lucida traces of individual cells showing neurons with stereotypical leading edge processes and trailing edge axons (arrows). CP, cortical plate; IZ, intermediate zone; SVZ, subventricular zone; VZ, ventricular zone; DIV, days *in vitro*.

(B) E19.5 neocortical slice from a *Tgfr2<sup>flox/flox</sup>* embryo electroporated at E14.5 with GFP and Cre. Top panel shows reduced neuronal migration 5 days after electroporation. Bottom panel contains camera lucida traces of individual cells showing cells with leading edge processes but no axons (arrows). Scale bars for (A) and (B): 100  $\mu$ m, top panels, 20  $\mu$ m bottom panels.

(C) Example images of labeled neurons from *Tgfr2<sup>flox/flox</sup>* embryos expressing GFP alone (left) or GFP plus Cre (right). Arrows indicate the presence (left) or absence (right) of axons. Arrowheads indicate the leading edge dendrite. Scale bar, 15  $\mu$ m.

(D) Magnified panels demarcated by white boxes in (A) and (B) showing the presence (left, GFP) or absence (right, Cre) of GFP-positive axon bundles parallel to the lateral ventricles. Scale bar, 30  $\mu$ m.

(E) Intracranial *ex vivo* electroporation in E14.5 embryos. After 3 DIV, most GFP-positive neurons are found in mid-migration within the IZ (right top). At 5 DIV, many neurons have reached the CP (right bottom). Magnified panels correspond to areas demarcated by white boxes. Scale bars: 100  $\mu$ m, left panels; 25  $\mu$ m, right panels.

(F) Organotypic neocortical slices from *Tgfr2<sup>flox/flox</sup>* embryos electroporated with GFP to label newborn neurons. Top panel shows neuronal migration after 5 days. Bottom panel contains camera lucida traces of individual cells showing cells with stereotypical leading edge processes and trailing edge axons (arrows).

(G) Organotypic neocortical slices from *Tgfr2<sup>flox/flox</sup>* embryos electroporated with GFP and Cre. Top panel shows GFP expression in CP, IZ, SVZ, and VZ. Bottom panel contains camera lucida traces of individual cells showing cells with leading edge processes but no axons (arrows). Scale bars for (A) and (B): 100  $\mu$ m, top panels, 20  $\mu$ m bottom panels.

(H) Example images of labeled neurons from *Tgfr2<sup>flox/flox</sup>* embryos expressing GFP alone (left) or GFP plus Cre (right). Arrows indicate the presence (left) or absence (right) of axons. Arrowheads indicate the leading edge dendrite. Scale bar, 15  $\mu$ m.

(I) Bar graph showing the percentage of cells with axons in WT and *Tgfr2*-KO embryos. WT is approximately 80% and *Tgfr2*-KO is approximately 30%.

(J) Time-lapse images of *Tgfr2<sup>flox/flox</sup>* E14.5 + GFP neurons at 0, 5, 10, 15, and 20 DIV.

(K) Time-lapse images of *Tgfr2<sup>flox/flox</sup>* E14.5 + Cre neurons at 0, 5, 10, 15, and 20 DIV.

(G) *Tgfb $\beta$ 2<sup>lox/lox</sup>* embryo electroporated to express GFP plus Cre in neuronal precursors. After 5 days, a subpopulation GFP-positive neurons reach the IZ, but many neurons fail to fully migrate (top panel). The bottom panel contains camera lucida traces showing individual cells with leading edge processes but lacking axons (arrows). Scale bars for (F) and (G): 100  $\mu$ m, top panels; 20  $\mu$ m, bottom panels.

(H) Example images of migrating neurons from *Tgfb $\beta$ 2<sup>lox/lox</sup>* embryos expressing GFP alone (left) or GFP plus Cre (right). Arrow indicates the presence (left) or absence (right) of axons. Arrowhead indicates the leading edge dendrite. Scale bar, 22  $\mu$ m.

(I) Quantification of cells containing axons in wildtype (WT, GFP expressing) and T $\beta$ R2-KO (T $\beta$ R2-KO, GFP plus Cre) neurons. Results were pooled from 2 embryos. n = 88, 92 cells for WT and T $\beta$ R2-KO, respectively. \*p<0.05, Student's t-test.

(J) Time-lapse imaging of neuronal migration and polarization in E15 *Tgfb $\beta$ 2<sup>lox/lox</sup>* embryos electroporated with GFP. The arrowhead marks the soma. The arrow marks the trailing axon. Time is indicated in min:sec. Scale bar, 20  $\mu$ m. See Movie S1.

(K) Time-lapse imaging of neuronal migration and polarization in E15 *Tgfb $\beta$ 2<sup>lox/lox</sup>* embryos electroporated with GFP plus Cre. The arrowhead marks the soma. The arrow indicates the expected location of axon formation, which is absent. Time is indicated in min:sec. Scale bar, 20  $\mu$ m. See Movie S1.



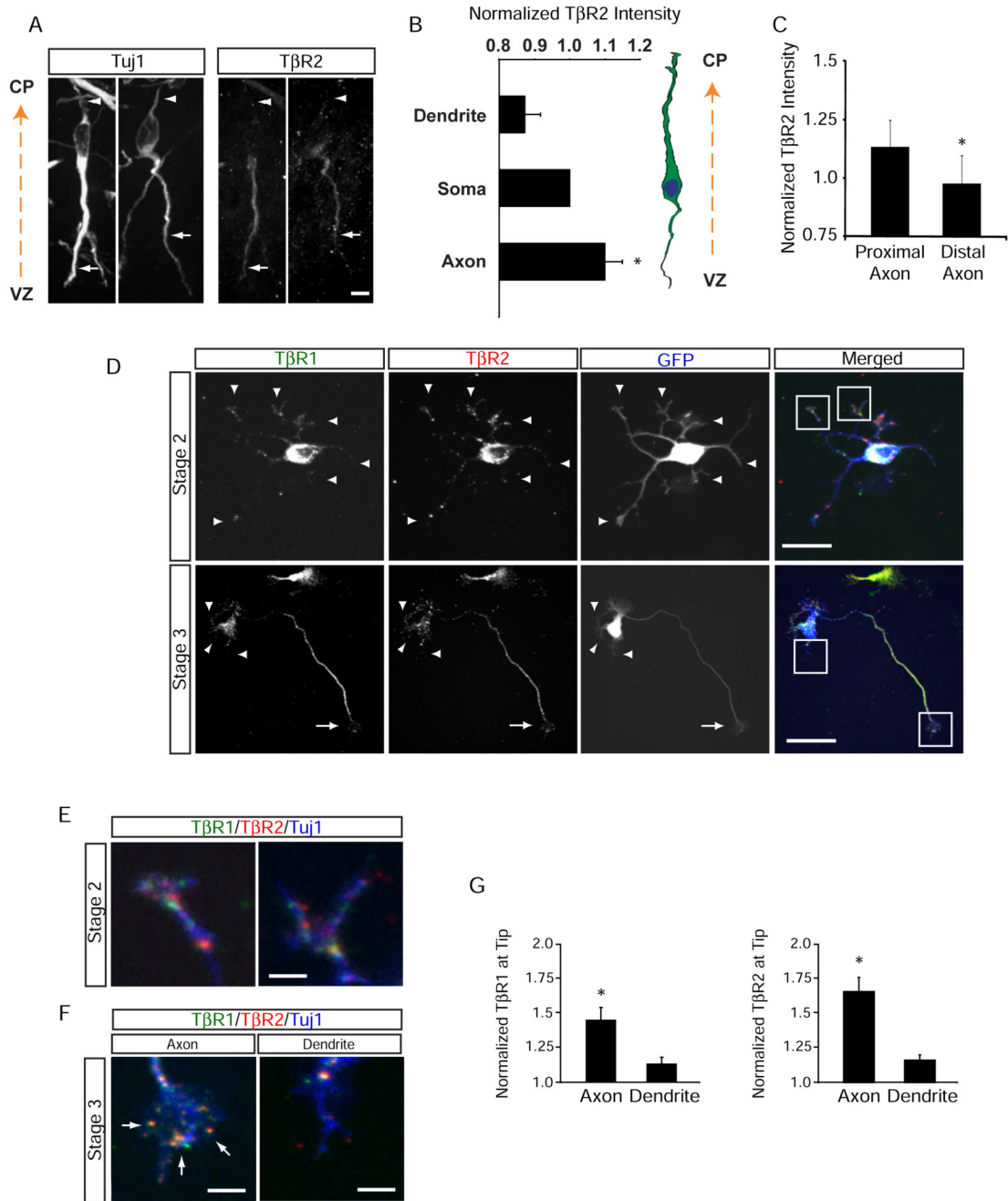


**Figure 3.**

**TGF-β Receptors Polarize to Nascent Axons**

(A) Enrichment of TβR2 in trailing-edge axons (arrows) of Tuj1-positive neurons migrating away from the ventricular zone (VZ) toward the cortical plate (CP) in an E14.5 mouse embryo. Arrowheads indicate the leading-edge dendrite. Scale bar, 20 μm.

(B) Quantitative analysis of TβR2 levels along migrating neocortical neurons. Linescans were performed to measure TβR2 immunofluorescence along the leading edge dendrite, soma, and trailing edge axon, n = 12.

(C) Quantitative analysis of TβR2 levels along axons, n = 12. \*p<0.05, Student's t-test. See Experimental Procedures for details.

(D) Surface-labeled T $\beta$ R1 and T $\beta$ R2 in dissociated E18 rat hippocampal neurons show punctate distribution at the tips of all neurites (arrowheads) in stage 2 cells prior to polarization (top panels). A few hours later during axon specification, both T $\beta$ R1 and T $\beta$ R2 become polarized to the axon in stage 3 neurons (arrows, bottom panels) while receptor staining is reduced in dendrites (arrowheads, bottom panels). Scale bars are 15  $\mu$ m for top panels and 20  $\mu$ m for bottom panels.

(E) Magnified panels demarcated by white boxes in the top right panel of (D) showing surface T $\beta$ R1 and T $\beta$ R2 staining at tips of undifferentiated stage 2 neurites. Scale bar, 3  $\mu$ m.

(F) Magnified panels demarcated by white boxes in the bottom right panel of (D) showing enriched T $\beta$ R1 and T $\beta$ R2 within the growth cone of the axon (left, arrows) and loss of surface receptor expression from the growth cone of a dendrite (right). Scale bar, 4  $\mu$ m.

(G) Integrated intensities of T $\beta$ R1 (left) and T $\beta$ R2 (right) immunofluorescence at the distal ends of axons and dendrites of stage 3 neurons. Values were normalized to the shortest neurite in each cell. n = 12 cells. \* p<0.05, Student's t-test.

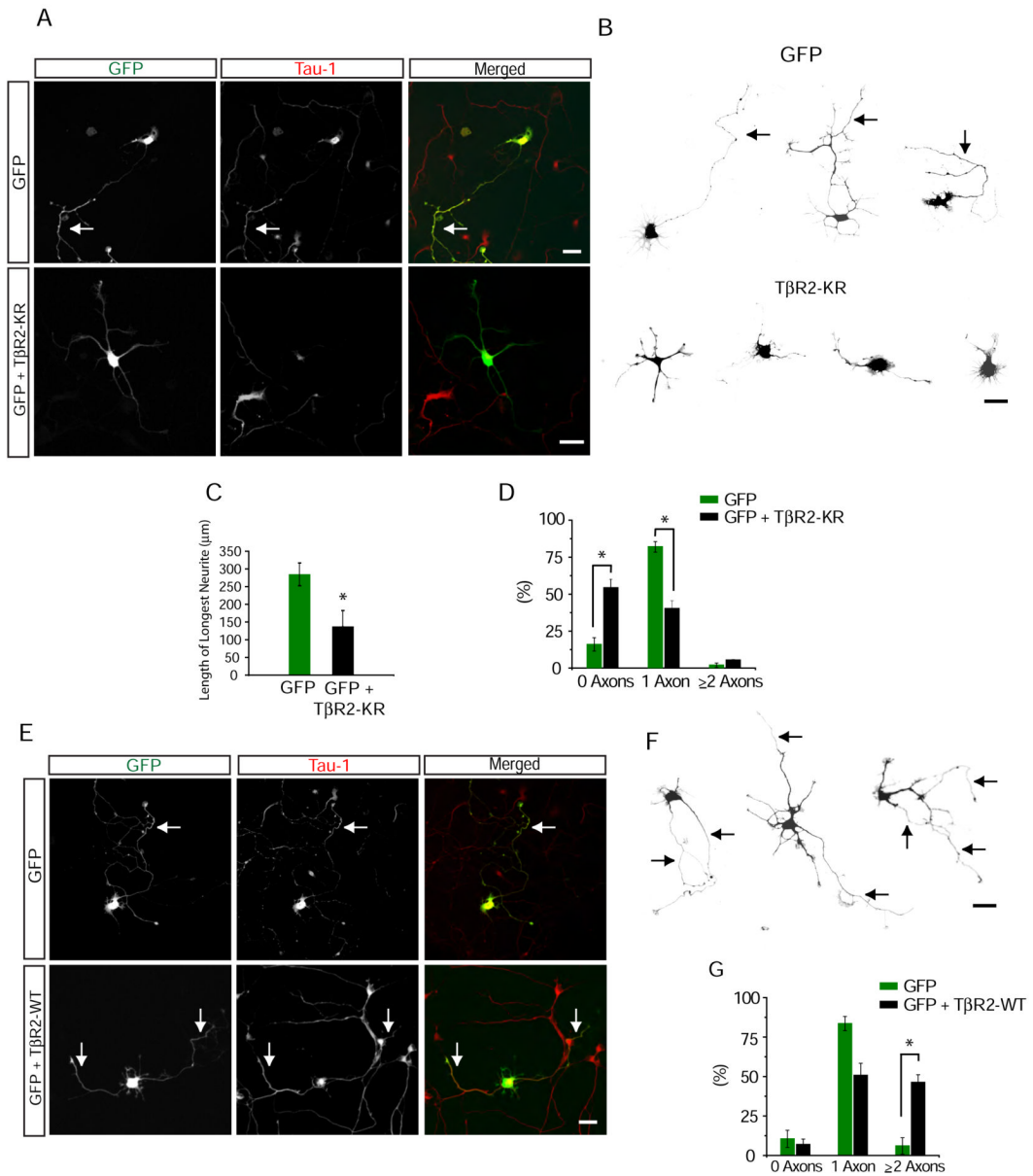


**Figure 4.**  
**Cell Autonomous TGF-β Signaling Mediates Axon Formation**  
 (A) Dissociated hippocampal neurons from E18 rat embryos expressing GFP or GFP + TβR2-KR were fixed and stained for the axonal marker tau-1. Cells were transfected 4-6 hours after plating and fixed 65-72 hours later. Arrow indicates tau-1 positive axons, which are absent from cells expressing TβR2-KR. Scale bar, 20 μm.  
 (B) Camera lucida traces of neurons expressing GFP (top) or GFP + TβR2-KR (bottom). Arrows indicate axons. Scale bar, 20 μm.  
 (C) Data represent means ± SEM of the longest neurite in control cells and cells expressing TβR2-KR. n = 12, \*p<0.05, Student's t-test.  
 (D) Quantification of axon number in cells expressing GFP alone or GFP + TβR2-KR. Data pooled from at least 3 independent experiments. GFP, n = 42; TβR2-KR, n = 53; \*p<0.05, Student's t-test.  
 (E) Similar to (A) but with GFP + TβR2-WT.  
 (F) Similar to (B) but with GFP + TβR2-WT.  
 (G) Similar to (D) but with GFP + TβR2-WT.

(E) Neurons expressing GFP or GFP + T $\beta$ R2-WT showing multiple tau-1 positive axons emerging from cells expressing T $\beta$ R2-WT (arrows). Scale bar, 20  $\mu$ m.

(F) Camera lucida traces of neurons expressing T $\beta$ R2-WT. Arrows indicate axons. Scale bar, 20  $\mu$ m.

(G) Quantification of axon number in cells expressing GFP alone or GFP plus T $\beta$ R2-WT. GFP, n = 41; T $\beta$ R2-WT, n = 44; \*p<0.05, Student's t-test.

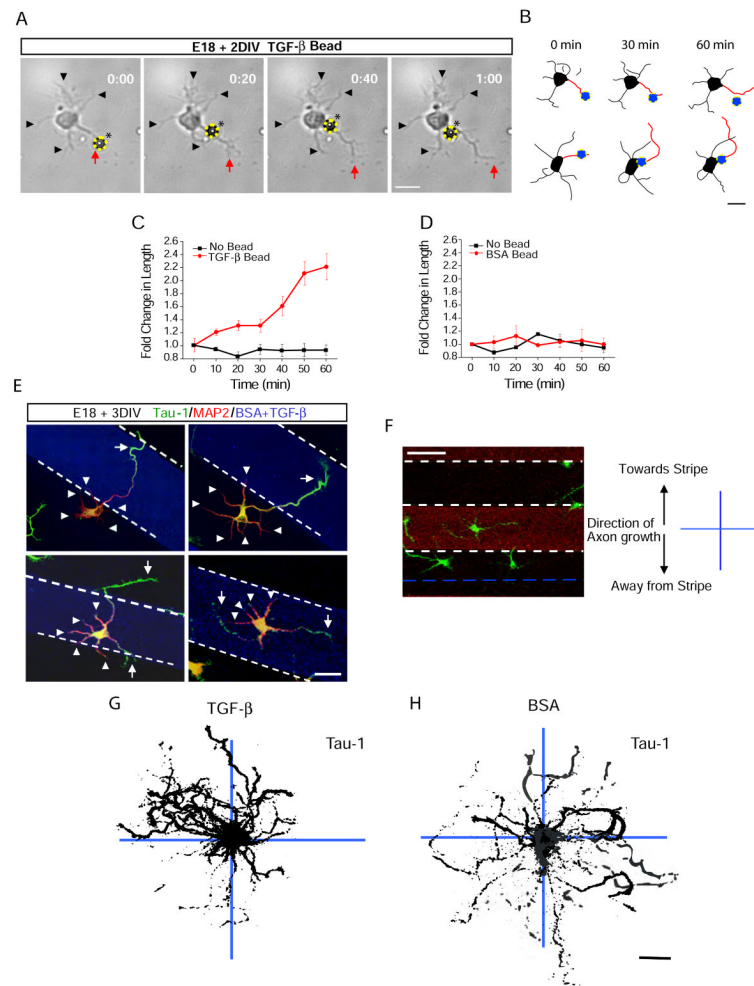


**Figure 5.**

**Local TGF- $\beta$  is Sufficient to Specify Axon Differentiation and Growth**

(A) Shown is an E18 + DIV 1 hippocampal neuron undergoing selective neurite extension. The yellow circle and asterisk labels a TGF- $\beta$ -conjugated bead. Black arrowheads indicate neurites untouched by beads. The red arrow indicates a neurite initially in contact with the bead. Times indicated in hours:minutes. Scale bar, 25  $\mu$ m. See Movie S2.

(B) Camera lucida traces of cells upon local TGF- $\beta$ -induced neurite growth. Neurites initially contacting TGF- $\beta$  beads (blue circles) are indicated in red. Scale bar, 25  $\mu$ m.

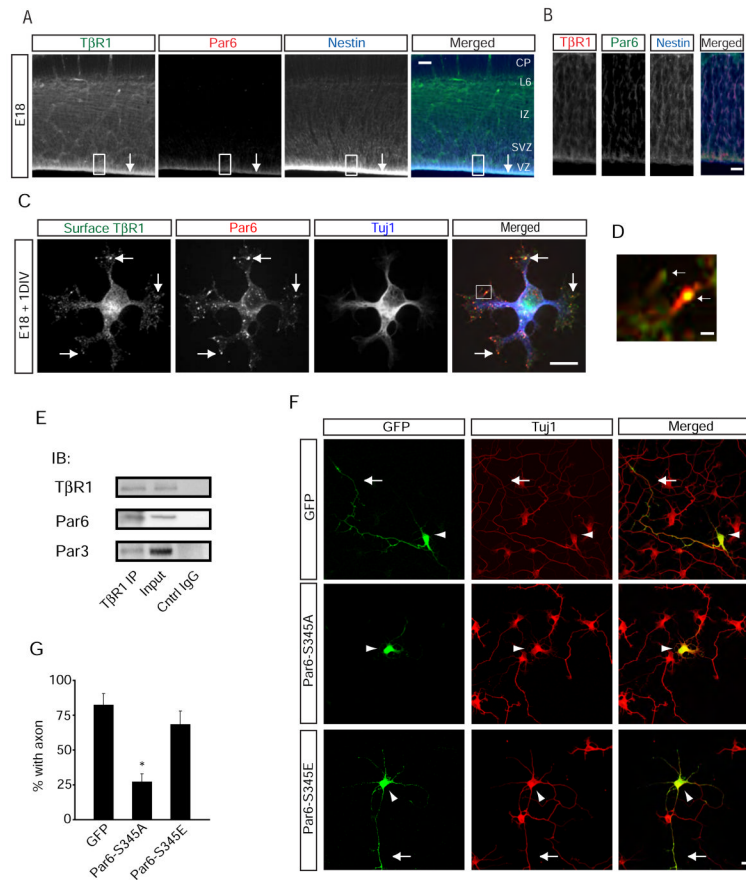
(C) Fold increase in the length of neurites either contacting (red) or not contacting (black) TGF- $\beta$  beads. Data represent means  $\pm$  SEM. n = 12.

(D) Fold increase in the length of neurites either contacting (red) or not contacting (black) BSA beads. Data represent means  $\pm$  SEM. n = 14.

(E) Localized TGF- $\beta$  spatially orients axon specification. Neurons were seeded on coverslips patterned with stripes of TGF- $\beta$ . After 48 h, cells were fixed and stained for tau-1 and MAP2 to visualize the axon (arrow) and dendrites (arrowheads), respectively. White dashed lines indicate the borders of the TGF- $\beta$  stripe. Scale bar, 50  $\mu$ m.

(F) For analysis, the 90  $\mu$ m space between stripes was bisected (blue dashed line). Tau-1 camera lucida traces of cells seeded next to stripes were mapped onto x-y coordinates where positive y values reflect the perpendicular direction toward the TGF- $\beta$  stripe and negative y values reflect the perpendicular direction away from the TGF- $\beta$  stripe. Scale bar, 50  $\mu$ m.

(G-H) Multiple overlaid camera lucida traces of tau-1 staining from neurons grown on TGF- $\beta$  (G) or BSA (H) striped coverslips. Individual cell traces shown in black. n = 45, 41. Scale bar, 25  $\mu$ m.

**Figure 6.****TGF- $\beta$ -Dependent Phosphorylation of Par6 is Required for Axon Formation**

(A) Co-localization of T $\beta$ R1 and Par6 at the VZ (arrow) of E17 mouse neocortex. Shown is immunohistochemical triple labeling for T $\beta$ R1, Par6, and the radial glial marker nestin. Scale bar, 50  $\mu$ m.

(B) Magnified image of the boxed region in (A) showing enriched expression of T $\beta$ R1 and Par6 in the VZ. Scale bar, 5  $\mu$ m.

(C) Immunocytochemistry for Par6 and surface T $\beta$ R1 in E18 dissociated rat hippocampal neurons. Arrows indicate colocalized puncta of Par6 and T $\beta$ R1 in neurite growth cones. Scale bar, 20  $\mu$ m.

(D) Magnification of box in (A) showing co-localization of T $\beta$ R1 clusters and Par6 in undifferentiated neurite tips. Scale bar, 2  $\mu$ m.

(E) Par6 and Par3 co-immunoprecipitate with T $\beta$ R1 in developing brain. E18 rat forebrain lysates were subjected to immunoprecipitation with a T $\beta$ R1 antibody, and co-precipitating proteins were immunoblotted for T $\beta$ R1, Par6, and Par3. Input lane represents 5% of the total protein quantity used for immunoprecipitation.

(F) Site-specific Par6 phosphorylation is required for axon differentiation. Hippocampal neurons were transfected with GFP, GFP-Par6-S345A, or GFP-Par6-S345E. Cells were fixed and analyzed for polarized growth. Whereas the majority of neurons expressing GFP and Par6-S345E possessed axons (arrow), neurons expressing Par6-S345A did not form distinguishable axons. Arrowhead marks the soma. Scale bar, 20  $\mu$ m.

(G) Data represent means  $\pm$  SEM of the percent neurons with an axon. GFP, n = 38; Par6-S345A, n = 34; Par6-S345E, n = 44. \*p<0.05, Student's t-test.

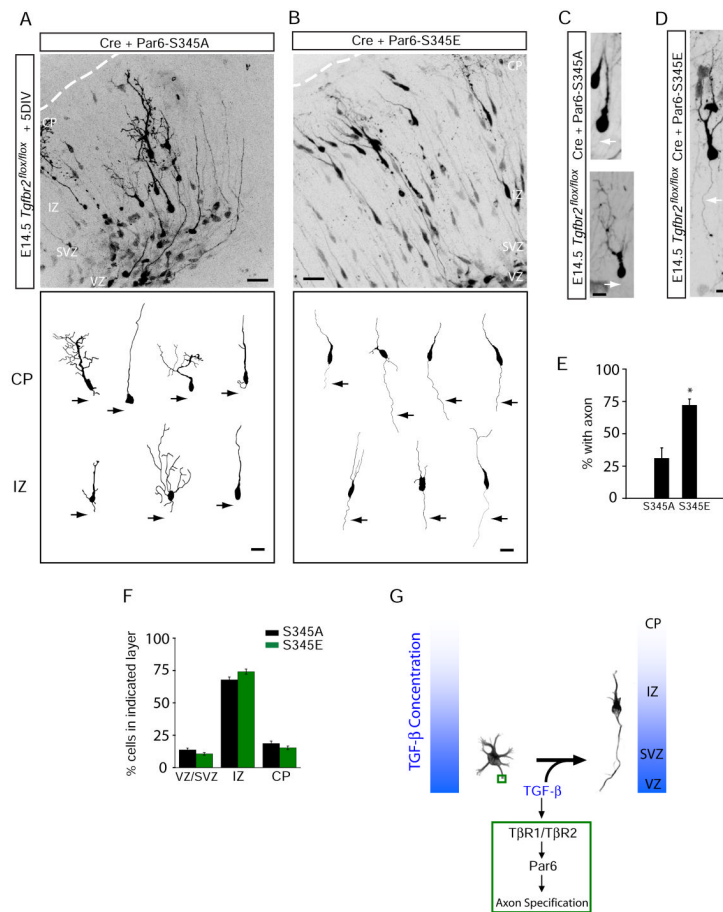


**Figure 7.**

**Phosphomimetic Par6-S345E Restores Axons in TβR2 KO Neurons *in Vivo***

(A) Neuronal progenitors in E15 *Tgfr2<sup>flox/flox</sup>* embryos were electroporated with Cre plus Par6-S345A and examined five days later. The bottom panel shows representative traces of neurons in the intermediate zone (IZ) and cortical plate (CP).

(B) A phosphomimetic mutant of Par6 rescues axon specification. Neuronal progenitors in E15 *Tgfr2<sup>flox/flox</sup>* embryos were electroporated with Cre plus Par6-S345E. The bottom panel shows representative traces of neurons in the IZ and CP. For (A) and (B), scale bars are 50 μm for top panels and 20 μm for bottom panels.

(C) Morphology of migrating TβR2-KO neurons expressing Par6-S345A, showing the absence of an axon (arrows). Scale bar, 22 μm.

(D) Morphology of a migrating TβR2-KO neuron expressing Par6-S345E showing the presence of a trailing axon (arrows). Scale bar, 22 μm.

(E) Data represent means ± SEM of the percent neurons with an axon. Experiments were averages from at 3-4 embryos. Par6-S345A, n = 89 cells; Par6-S345E, n = 84; \*p<0.05, Student's t-test.

(F) Quantitative analysis of migration defects in TβR2-KO neuron expressing Par6-S345A or Par6-S345E. Par6-S345E did not rescue migration defects caused by the loss of TGF-β signaling. Compare to Figure S2D. Results represent experiments from at least 4 embryos. n = 2357, 4598 cells for Par6-S345A and Par6-S345E, respectively. See Supplemental Methods for details.

(G) A model for TGF-β-dependent axon specification in developing neocortex. VZ, ventricular zone; IZ, intermediate zone; CP, cortical plate.